Engineered Electrical Conduction Tract Restores Conduction in Complete Heart Block

From In Vitro to In Vivo Proof of Concept

Eugenio Cingolani, MD,* Vittoria Ionta, PHD,*† Ke Cheng, PHD,* Alessandro Giacomello, MD, PHD,†
Hee Cheol Cho, PHD,* Eduardo Marbán, MD, PHD*

ABSTRACT

BACKGROUND Cardiac electrical conduction delays and blocks cause rhythm disturbances such as complete heart block, which can be fatal. Standard of care relies on electronic devices to artificially restore synchrony. We sought to create a new modality for treating these disorders by engineering electrical conduction tracts designed to propagate electrical impulses.

OBJECTIVES This study sought to create a new approach for treating cardiac conduction disorders by using engineered electrical conduction tracts (EECTs).

METHODS Paramagnetic beads were conjugated with an antibody to gamma-sarcoglycan, a cardiomyocyte cell surface antigen, and mixed with freshly isolated neonatal rat ventricular cardiomyocytes. A magnetic field was used to pattern a linear EECT.

RESULTS In an in vitro model of conduction block, the EECT was patterned so that it connected 2 independently beating neonatal rat ventricular cardiomyocyte monolayers; it achieved coordinated electrical activity, with action potentials propagating from 1 region to the other via EECT. Spiking the EECT with heart-derived stromal cells yielded stable structures with highly reproducible conduction velocities. Transplantation of EECTs in vivo restored atrioventricular conduction in a rat model of complete heart block.

CONCLUSIONS An EECT can re-establish electrical conduction in the heart. This novel approach could, in principle, be used not only to treat cardiac arrhythmias but also to repair other organs. (J Am Coll Cardiol 2014;64:2575–85)
© 2014 by the American College of Cardiology Foundation.

Cardiac electrical conduction delays and blocks are associated with various rhythm disturbances (1), notably complete heart block (i.e., third-degree atrioventricular [AV] block), which can be lethal. Conduction delays can also create a substrate for re-entrant arrhythmias such as ventricular tachycardia (2). Current therapies depend on electronic pacemakers in the case of heart block or ablative therapies targeting strands of slowly conducting viable myocardium to terminate re-entrant circuits in tachyarrhythmias (3). Both strategies are suboptimal. Electronic pacemakers are associated with multiple risks, including an abnormal ventricular activation pattern clinically associated with a

ABBREVIATIONS AND ACRONYMS

AV = atrioventricular

CDCs = cardiosphere-derived cells

CV = conduction velocity

Cx = connexin

EDAC = 1-ethyl-3-(3-dimethylaminopropyl) carbodiimide

EECT = engineered electrical conduction tract

EECT-C = cardiosphere-derived cell-enriched engineered electrical conduction tract

EGMs = electrograms

GFP = green fluorescent protein

NRVMs = neonatal rat ventricular myocytes

progressive decline in pump function (4,5). Ablation destroys living heart tissue and, in ventricular tachycardia, is associated with significant morbidity and mortality (6-8).

Our goal was to create a new approach to treating such disorders by using engineered electrical conduction tracts (EECTs) designed to bridge or bypass zones of impaired conduction. We report a highly generalizable means of creating these EECTs by using magnetic patterning to orient cells conjugated to paramagnetic microbeads. As proof of concept, we showed that EECTs can re-establish electrical conduction between disconnected regions of 2-dimensional cardiac tissue and in an animal model of complete heart block.

METHODS

FORMATION OF CELL-TARGETED PARAMAGNETIC BEADS.
Paramagnetic fluorescent microspheres (8 μm in diameter; Bangs Laboratories, Inc., Fishers, Indiana) were conjugated with gamma-sarcoglycan antibody (200 μg; Santa Cruz Biotechnology, Dallas, Texas) or with CD105 antibody (200 μg; R&D Technologies, North Kingstown, Rhode Island) by using the PolyLink Protein Coupling Kit (Bangs Laboratories) according to the manufacturer's instructions. In brief, carboxyl-modified polymer-based microspheres were resuspended in PolyLink coupling buffer and activated by addition of 1-ethyl-3-(3-dimethylaminopropyl)carbodiimide (EDAC). Covalent binding of the specific antibody to the surface of the activated microspheres was achieved by incubating 200 μg of either gamma-sarcoglycan or CD105 antibodies at room temperature for 2 h. Antibody-coated microspheres were resuspended in PolyLink Wash/Storage buffer and stored at 4°C for subsequent experiments.

CARDIOMYOCYTE ISOLATION, CULTURE, AND CONJUGATION.
Neonatal rat ventricular myocytes (NRVMs) were isolated from 1- to 2-day-old pups as described (9). We created a 2-dimensional conduction block model by plating NRVMs in a culture plate, then scraping along the middle of the monolayer. Complete conduction block was confirmed 24 h after mechanical interruption by verifying asynchronous beating of the 2 independent monolayers. Freshly isolated NRVMs (2×10^6) were incubated in suspension with gamma-sarcoglycan antibody-coated paramagnetic microspheres for 4 h at room temperature by using a 1:1 ratio of cells to microspheres. The newly

formed NRVM-microsphere complexes were subsequently used for EECT construction.

CARDIOSPHERE-DERIVED CELL CULTURE AND CONJUGATION.
Human cardiosphere-derived cells (CDCs) were isolated from heart biopsy specimens and cultured as described (10). CDCs were incubated in suspension with CD105 antibody-coated microspheres for 4 h at room temperature by using a 1:1 ratio of cells to microspheres. The newly formed CDC-microsphere complexes were used for construction of modified EECT (cardiosphere-derived cell-enriched engineered electrical conduction tracts [EECT-C]).

CONSTRUCTION OF EECT IN SITU WITH MAGNETIC FIELD.
To re-establish conduction between the 2 halves of the interrupted NRVM monolayer, an EECT was created by exposing NRVM-microsphere complexes (2×10^6 cells in a 1:1 ratio of cells to microspheres) to a linear magnetic field aligned perpendicularly to the axis of interruption. After 12 h, the cells were removed from the magnetic field, and the culture plate was returned to the incubator (Online Figure 1). To enhance the physical integrity of the EECT, the NRVM-microsphere complexes were mixed with the CDC-microsphere complexes and plated over a linear magnetic field to create EECT-C. For in vivo transplantation, NRVM-microsphere complexes were plated in an ultralow attachment plate (Corning Life Sciences, Tewksbury, Massachusetts) and were then exposed for 12 h in the incubator to a linear magnet placed underneath the plate. Nonadherent EECTs were created by exposing the NRVM-microsphere complexes (5×10^6 NRVMs in a 1:1 cell to microsphere ratio) to the magnetic field.

HIGH-RESOLUTION OPTICAL MAPPING.
Action potential propagations were recorded on a 469-photodiode array system (WuTech Instruments, Gaithersburg, Maryland) by using a voltage-sensitive dye. Cells were incubated with di-4-ANEPPS (50 μM; Invitrogen Corporation, Carlsbad, California) for 2 min at 37°C, followed by dye washout. To prevent motion artifacts, recordings were obtained at room temperature in Ca^{+2}-free Tyrode's solution containing blebbistatin (10 μM; Sigma-Aldrich Co., St. Louis, Missouri). Action potential duration and conduction velocity (CV) across the NRVM monolayers and the EECT were analyzed with NeuroPlex software (RedShirtImaging, L.L.C., Decatur, Georgia).

IMMUNOMICROSCOPY AND CONFOCAL MICROSCOPY.
For immunohistochemistry, EECTs were fixed overnight with 4% paraformaldehyde, permeabilized, and blocked with Dako protein block solution (Dako, Carpinteria, California) containing 1% saponin
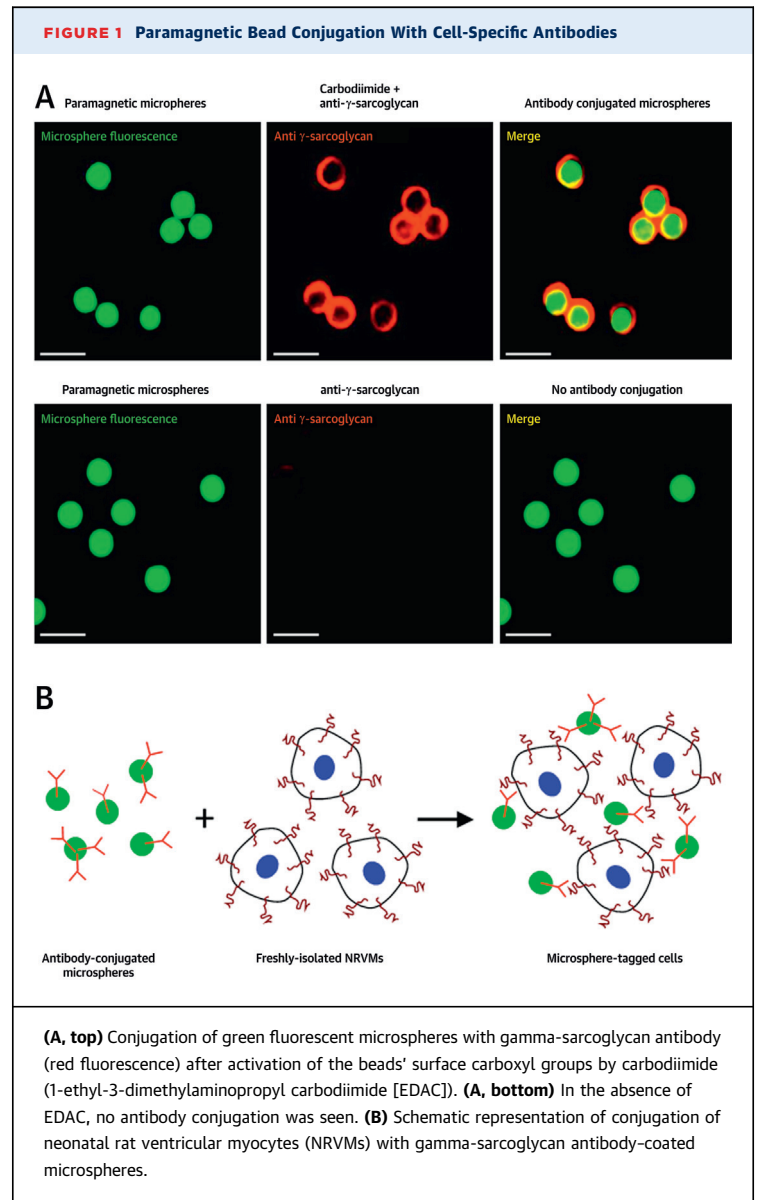
(Sigma-Aldrich) for 1.5 h. Immunostaining was performed with primary antibodies against the following molecules: connexin (Cx) 43 (rabbit, 1:200; Abcam plc, Cambridge, Massachusetts) and sarcomeric alpha-actinin (mouse, 1:400; Sigma-Aldrich). Nuclear staining was performed with 4′,6-diamidino-2-phenylindole, and microspheres were identified by their inherent green fluorescence. Incubation of secondary antibodies conjugated to Cy5 (1:400; Abcam) or Texas Red (1:400, Abcam) was performed at room temperature. Images were obtained by using a confocal microscope (TCS SP5 X, Leica Microsystems, Wetzlar, Germany).

To demonstrate in vivo structural integration, rats were transplanted with EECT-C transduced before EECT-C construction with an adenovirus-encoding green fluorescent protein (GFP). Hearts were harvested 72 h after transplantation, washed with phosphate-buffered saline, and fixed with 4% paraformaldehyde. After overnight incubation with 15% sucrose, hearts were preserved in optimum cutting temperature for cryosectioning. Slides were permeabilized and blocked with Dako protein block solution (Dako) for 1.5 h. Immunostaining was performed with the following primary antibodies: Cx43 (rabbit, 1:100; Abcam), sarcomeric alpha-actinin (mouse, 1:100; Sigma-Aldrich), and GFP (goat, 1:50; Abcam). Nuclei were stained with 4′,6-diamidino-2-phenylindole, and paramagnetic spheres were identified by their inherent green fluorescence. Incubation with Alexa Fluor 488 donkey anti-goat immunoglobulin G, Alexa Fluor 568 goat anti-mouse immunoglobulin G, or Alexa Fluor 647 goat anti-rabbit immunoglobulin G (1:400, Life Technologies, Grand Island, New York) secondary antibodies (Life Technologies) at 1:400 was performed at room temperature. Images were obtained by using a confocal microscope (TCS SP5 X, Leica Microsystems).

SCANNING ELECTRON MICROSCOPY. Scanning electron microscopy was used to visualize the morphological details of the EECT 3-dimensional structure. Samples were fixed with 2% glutaraldehyde in 0.1 M of sodium cacodylate (pH 7.2) for 1 h, then dehydrated by using progressive ethanol concentrations (35%, 50%, 70%, 80%, 95%, and 100%) for 10 min each and dried in hexamethyldisilazane (Sigma-Aldrich). Scaffolds were sputter-coated with gold and images were captured with a LEO-982 scanning electron microscope (LEO Corporation, Oberkochen, Germany).

IN VIVO TRANSPLANTATION OF ECCT-C. Adult Sprague Dawley rats (∼220 g) were anesthetized by using isoflurane (4% induction, 1.5% maintenance),

intubated, and mechanically ventilated. A left thoracotomy was performed to expose the heart and the AV groove for direct visualization. Upon removal of the pericardium, a pre-formed EECT-C was laid on top of the heart, connecting the epicardial surfaces of the right atrium and the right ventricle. The proximal and distal ends of the EECT-C were affixed to the right atrium and right ventricle with fibrin glue; no additional pretreatment was performed at the attachment points. After confirming the mechanical stability of the implanted EECT-C, the chest was closed. Animals were reanesthetized 3 days later for in vivo surface electrocardiograms, followed by euthanasia and heart harvest. Given the rapid

FIGURE 1 Paramagnetic Bead Conjugation With Cell-Specific Antibodies

(A, top) Conjugation of green fluorescent microspheres with gamma-sarcoglycan antibody (red fluorescence) after activation of the beads' surface carboxyl groups by carbodiimide (1-ethyl-3-dimethylaminopropyl carbodiimide [EDAC]). **(A, bottom)** In the absence of EDAC, no antibody conjugation was seen. **(B)** Schematic representation of conjugation of neonatal rat ventricular myocytes (NRVMs) with gamma-sarcoglycan antibody–coated microspheres.

turnover of Cxs (11,12), the 3-day time point was chosen to allow the EECT-C to be stably engrafted and electrically coupled with the heart, while minimizing rejection of the donor tissue construct. Harvested whole hearts were mounted on a retrograde Langendorff perfusion system for recording of surface electrograms (EGMs) through epicardial electrodes connected to a digital recording system (ADInstruments, Colorado Springs, Colorado). Preparations that exhibited viability and persistent attachment of the EECT-C were used for analysis.

To assess conduction through the EECT-C, the AV node was blocked pharmacologically by adding methacholine (10 mg/ml) to the perfusate. To assay AV conduction, the right atrium or right ventricle wa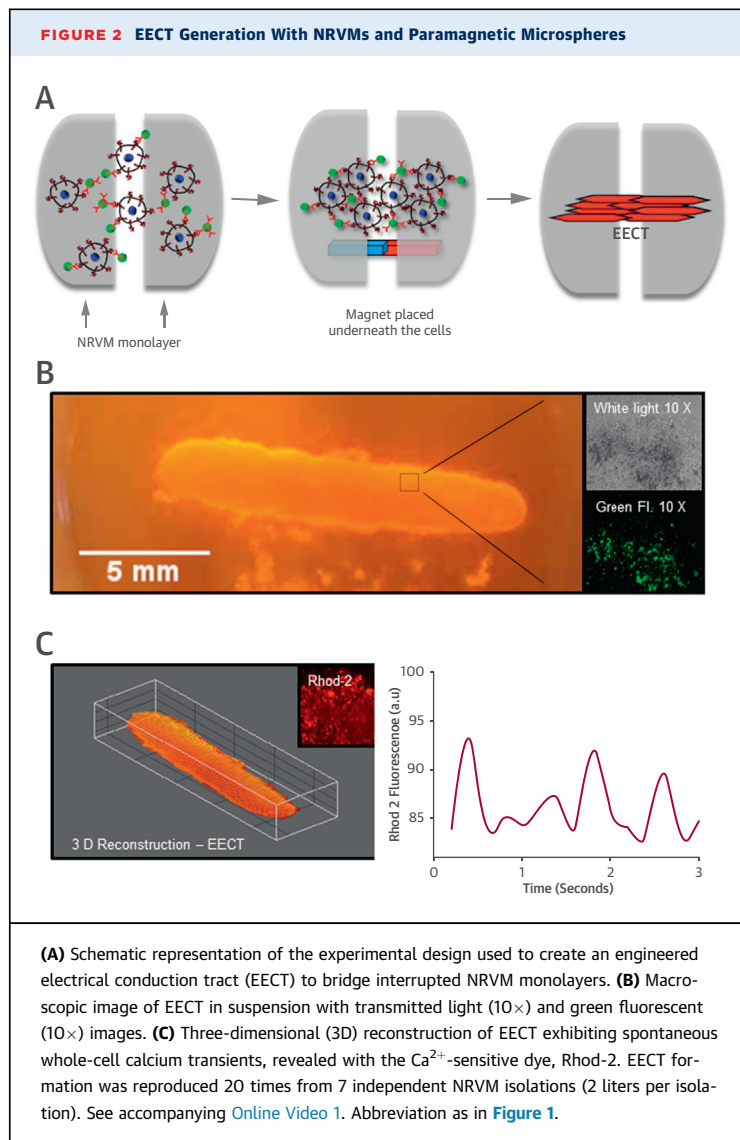s paced through epicardial platinum electrodes connected to an isolated pulse stimulator (A-M Systems, Sequim, Washington). Animals were subjected to sham operation (no EECT-C) or –EECT-C transplantation. Investigators were not blinded to the group allocation. All animal experiments were performed in compliance with the Cedars-Sinai Institutional Animal Care and Use Committee guidelines.

STATISTICAL ANALYSIS. Statistical significance was calculated by using 2-way analysis of variance or the Student *t* test when appropriate. Unless specified otherwise, all data are presented as mean ± SEM. A p value <0.05 was considered statistically significant.

RESULTS

CREATION OF AN EECT. The study concept was to form a complex of cardiomyocytes with paramagnetic beads whose surface is covalently conjugated to a cardiomyocyte-specific antibody. Affinity binding of cardiomyocytes to the beads enables patterning of the complex into a defined structure by attracting the beads with a magnetic field. Paramagnetic beads 8 μm in diameter were activated by EDAC, forming covalent bonds between the free carboxyl groups on the beads' surfaces and the amide groups on EDAC (**Figure 1A**). Primary antibodies were then conjugated to the activated microspheres via peptide bonds between amino-terminal groups of the antibody and carboxyl groups on the microsphere surface. This antibody-microsphere conjugation step depends on the catalytic activity of the EDAC; in its absence, nonspecific primary antibody binding to the beads is undetectable (**Figure 1B**). The microspheres are manufactured to emit green fluorescence for detection under fluorescence microscopy.

An ideal cell substrate for EECT constructs should have high cell-cell electrical coupling within the EECT and at the ends where the EECT contacts the host tissue. In addition, the cell substrate should be terminally differentiated so that the EECT retains its conduction properties and shape. For proof of concept, NRVMs satisfy these criteria and thus were chosen as the EECT cell substrate. A number of cardiomyocyte cell surface antigens were tested for their ability to bind to NRVMs, including integrins (alpha and beta), cadherins (N, E, and I), Cx43 and Cx40, and sarcoglycans. Among them, gamma-sarcoglycan-conjugated microspheres exhibited the highest binding efficiency and specificity for NRVMs. Sarcoglycans are integral membrane proteins connecting the contractile apparatus to the extracellular matrix (13-15). Placing a linear magnet underneath a suspension of the NRVM–microsphere complex formed an EECT (**Figures 2A and 2B**). Within 24 h, the

FIGURE 2   EECT Generation With NRVMs and Paramagnetic Microspheres

(A) Schematic representation of the experimental design used to create an engineered electrical conduction tract (EECT) to bridge interrupted NRVM monolayers. **(B)** Macroscopic image of EECT in suspension with transmitted light (10×) and green fluorescent (10×) images. **(C)** Three-dimensional (3D) reconstruction of EECT exhibiting spontaneous whole-cell calcium transients, revealed with the Ca^{2+}-sensitive dye, Rhod-2. EECT formation was reproduced 20 times from 7 independent NRVM isolations (2 liters per isolation). See accompanying Online Video 1. Abbreviation as in **Figure 1**.

EECT demonstrated rhythmic, syncytial contractions (Online Video 1), indicating that cell-cell electrical coupling was established within the spontaneously active construct (16). Global electrical coupling in the EECT is further demonstrated in **Figure 2C**, which illustrates spontaneous intracellular Ca^{2+} transients measured from a 1-mm^2 area of the EECT.

EECT BRIDGES CONDUCTION BETWEEN 2 MONO-LAYERS OF NRVMS.

To test if the EECT could relay electrical signals, we created an in vitro model of conduction block by mechanically disrupting the NRVM monolayers, thus creating 2 independently beating halves (**Figure 3A**). To re-establish conduction, EECTs were formed in situ by placing a magnet perpendicular to the axis of interruption (**Figure 3B**). Within 1 day of EECT formation, the 2 NRVM islands beat in tandem, and the action potentials propagated from 1 island to the other via EECT, with a mean CV of 18 ± 4 cm/s. Action potential morphology and action potential duration at 90% of repolarization were similar in the EECT (443 ± 5 ms) and the adjacent monolayers (439 ± 12 ms; p = NS). NRVMs cultured as monolayers exhibited occasional spontaneous contractions (17), accounting for the irregular beating shown in **Figure 3B**. To control for nonspecific bridging of the 2 NRVM islands, EECTs were formed parallel to the axis of the monolayer interruption (**Figure 3C**). No synchronous beating occurred between the 2 NRVM islands, indicating that the bridging of electrical conduction by EECTs is specific, occurring only when EECT termini physically contact the disconnected tissues.

THE ADDITION OF CARDIAC STROMAL CELLS AUGMENTS CELL VIABILITY AND ELECTRICAL CONDUCTION PROPERTIES OF THE EECT.

The EECT used in **Figure 2** was composed of NRVMs and beads only. Although capable of bridging a conduction gap (**Figure 3**), the structure was fragile, which gave rise to large SDs in EECT conduction velocities. We thus examined if admixing the NRVMs with another cell type might stabilize the structures. Antibody-mediated cell attachment to paramagnetic microspheres allows incorporation of different cell types by using cell type-specific antibodies. CDCs are CD105$^+$ stromal cells derived from myocardial biopsy specimens (10) that electrically couple to and exert antiapoptotic effects on cardiomyocytes (10,18). In the native heart, the majority of total cardiac cells are nonmyocytes and provide structural support (19-21); we thus reasoned that addition of CDCs might enhance NRVM viability and/or modulate EECT conduction properties.

To this end, CDCs were bound to CD105-conjugated microspheres and mixed with NRVMs

bound to gamma-sarcoglycan-conjugated microspheres. Electron micrographs revealed that EECTs constructed with either 2% or 10% CDCs (EECT-C2 or EECT-C10, respectively) exhibited substantially more extracellular matrix than EECTs (**Figure 4A**). EECT-C10 demonstrated a high degree of Cx43-mediated gap junction coupling at cell-cell borders (yellow arrowheads, **Figure 4B**) and higher cell viability (**Figure 4C**) than EECTs. Measurements of CV by using optical mapping indicated that NRVM-only EECTs conduct at a highly variable velocity of 21.9 ± 19 cm/s (n = 4). Addition of either 2% or 10% CDCs decreased

FIGURE 3 Restoration of Conduction in a 2-Dimensional Model of Conduction Block

(A) Optical mapping recordings demonstrate independent activation of interrupted NRVM monolayers. **(B)** Restoration of conduction block with simultaneous activation of the 2 NRVM monolayers after EECT implantation. **(C)** Implantation of EECT parallel to NRVM monolayers results in asynchronous activation of the 2 NRVM monolayers. Experiments were reproduced 4 times from 3 independent NRVM isolation procedures (2 liters per isolation). Abbreviations as in **Figures 1 and 2**.
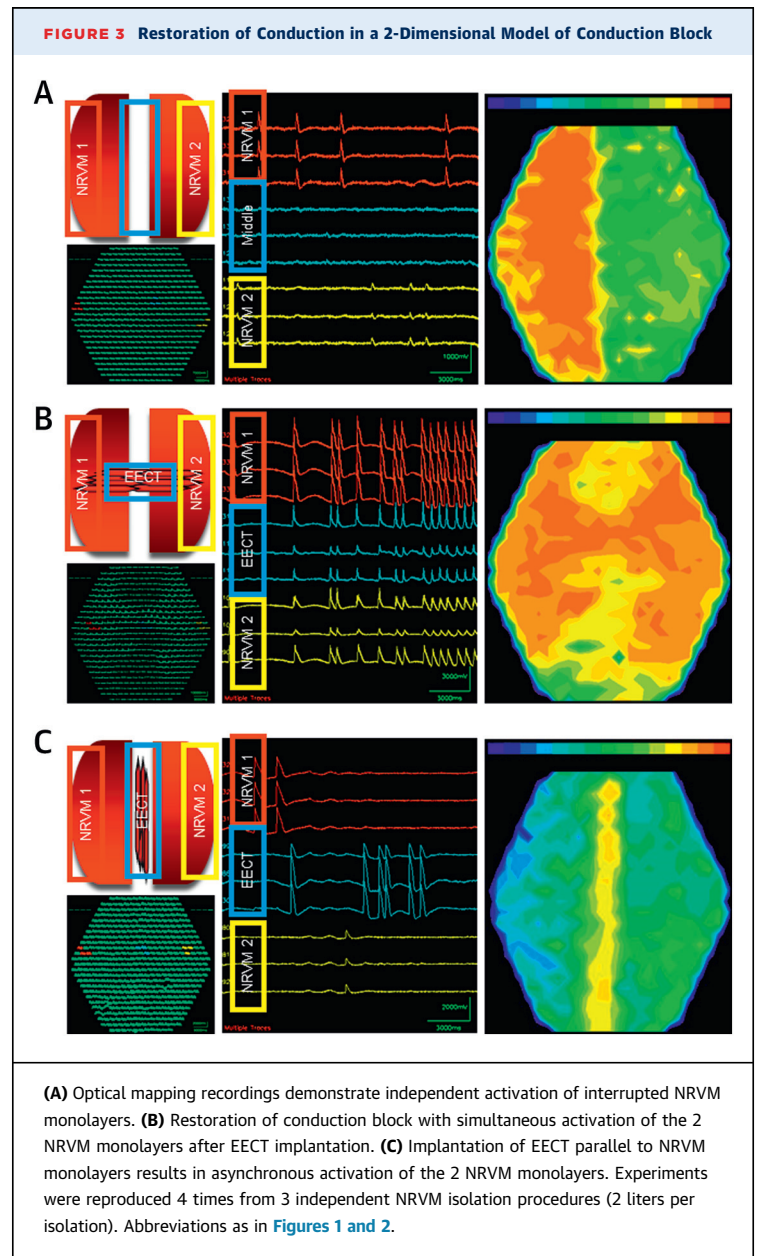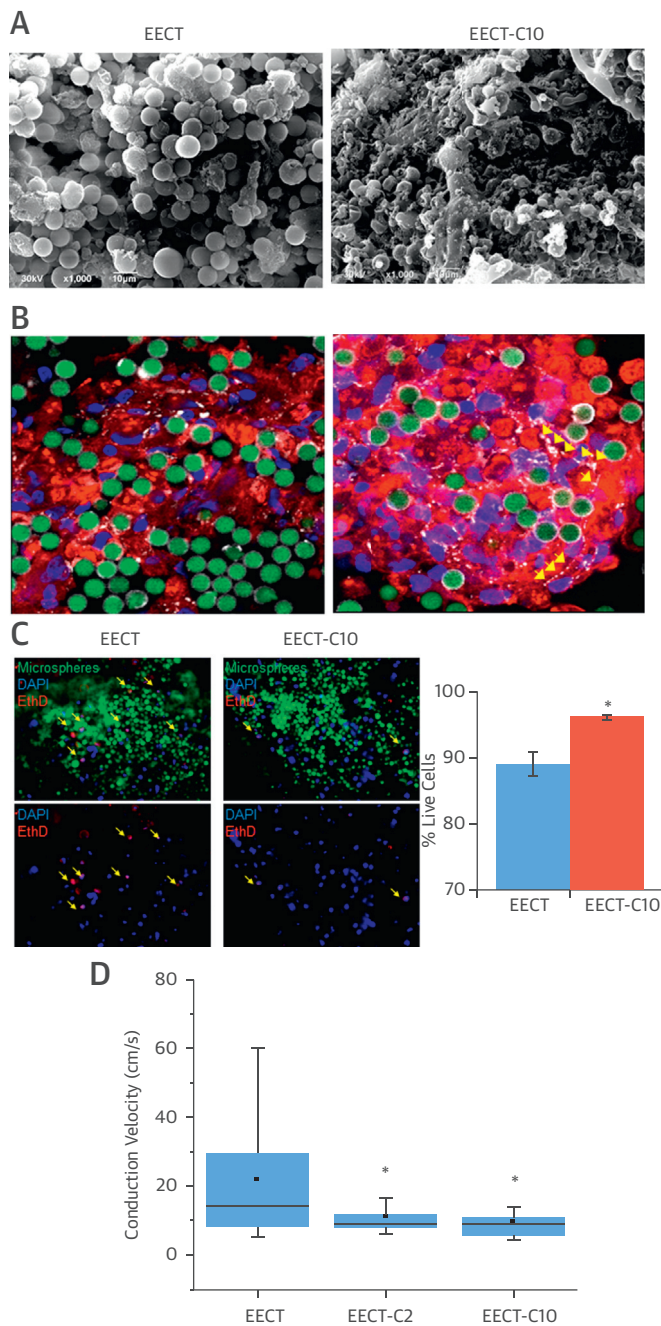
FIGURE 4 Addition of 10% CDCs to EECT (EECT-C10) Enhances Structural Integrity and Improves Viability of EECT in Culture

(A) Electron microscopy images of EECT (left) and EECT-C10 (right). (B) Immunohistochemistry of EECT (left) and EECT-C10 (right). Green: microspheres; red: sarcomeric actin; white: connexin 43; blue: 4′,6-diamidino-2-phenylindole (DAPI) nuclei. (C) Representative images of ethidium homodimer staining of EECT and EECT-C10 (left) and quantification of percent live cells (right). (D) Addition of cardiosphere-derived cells (CDCs) to EECT results in less variability in conduction velocity. In each experimental group, n = 3 biological replicates. Error bars represent SDs. *p < 0.05 according to 2-way analysis of variance. Abbreviation as in Figure 2.

the mean CVs (11.1 ± 7 cm/s and 8.7 ± 5 cm/s, respectively). This finding is not surprising; CDCs can couple to NRVMs and other CDCs via gap junctions (10) but are themselves inexcitable, acting as electrical sinks. More importantly, EECT-C2 and EECT-C10 exhibited substantially more consistent CV measurements, with almost 3-fold lower SDs (Figure 4D). The uniformly lower CVs also render EECT-C2 and EECT-C10 as favorable AV node surrogates, avoiding complications associated with rapidly conducting accessory pathways (22). These findings indicate that the addition of CDCs to EECTs renders the construct more consistent in structure and function.

EECT-C RE-ESTABLISHES CONDUCTION FROM THE ATRIA TO THE VENTRICLES IN A MODEL OF COMPLETE HEART BLOCK.

We tested the ability of EECT-C to function in the intact heart in a rat model of complete heart block. We sought to first create an accessory tract for conduction between the atria and the ventricles by using EECT-C and then to verify that the EECT could sustain conduction upon suppression of the AV node. For these experiments, we constructed EECT-C10 on a mesh of 30-μm pore size; we then implanted it by affixing 1 end of the mesh onto the right atrium and the other end onto the anterior surface of the right ventricle of the adult rat heart by using fibrin glue. Surface electrocardiograms of EECT-C10-implanted animals 72 h later showed an increase in QRS interval duration compared with nonimplanted control rats (15.8 ± 0.4 ms vs. 12.8 ± 0.3 ms; p < 0.05 [n = 3 each group]) (Figure 5A). This outcome verifies creation of a functional accessory tract, as in Wolff-Parkinson-White syndrome (23), albeit without accelerated AV conduction (no significant differences in PR interval duration) (Figure 5B).

After in vivo electrocardiogram recordings, hearts were explanted and fixed with retrograde perfusion for recording of surface EGMs (n = 2). Infusion of methacholine created complete heart block and slowed the sinus rate (prolongation of A-A interval), leading to sinus arrest (top panel, Figure 5C). To test conduction via the EECT-C10 upon methacholine-induced AV block, the right atrium was paced electrically, leading to faithful 1:1 capture of the ventricles, as demonstrated by the presence of a ventricular EGM (V) following each atrial EGM (A) and the atrial pacing deflection (P) (bottom panel, Figure 5C). To confirm that the recorded conduction was indeed through the EECT, recordings were repeated after mechanical disruption of the implanted EECT. No evidence of ventricular activity was seen after
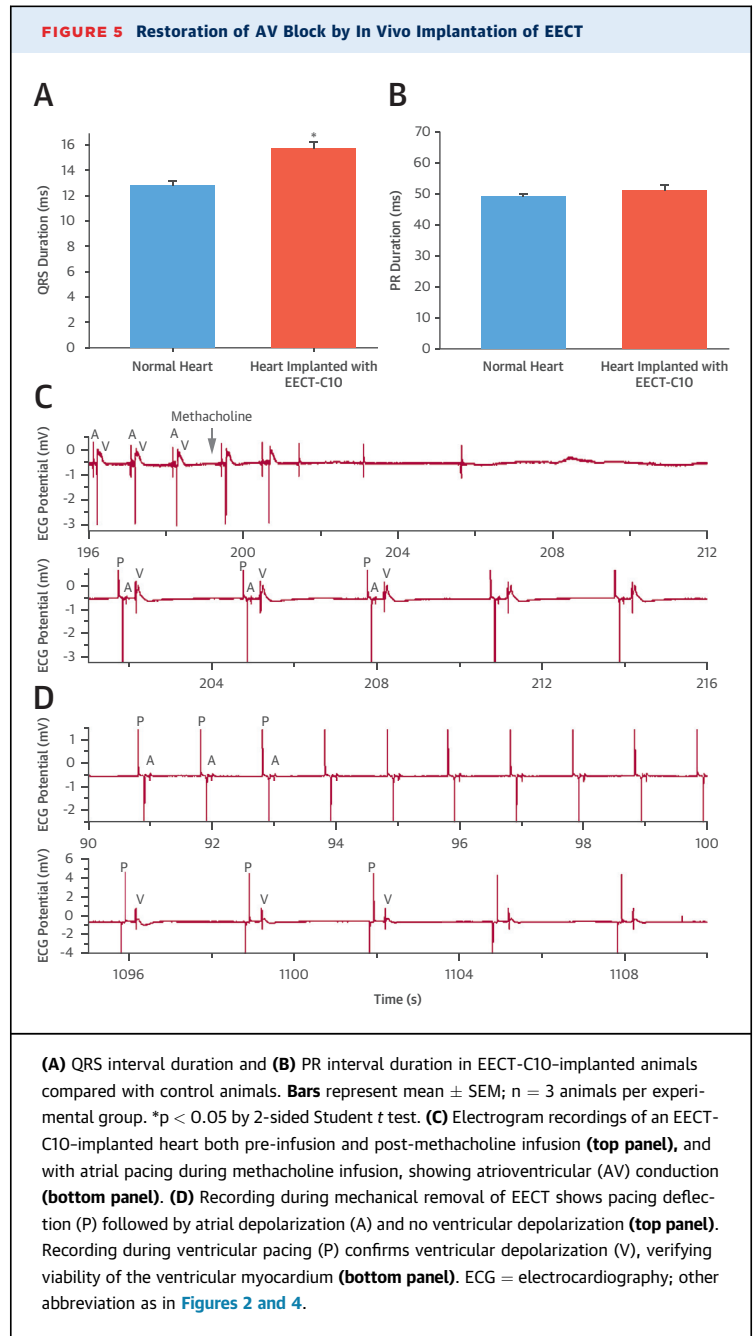
EECT removal (top panel, **Figure 5D**). Viability of the ventricular myocardium was verified by the ability to capture the ventricle with a pacing electrode (bottom panel, **Figure 5D**). Taken together, our data show that EECT can support functional A-V conduction in the intact heart in a model of complete heart block.

IN VIVO INTEGRATION OF EECT-C THROUGH GAP JUNCTIONS. Integration of EECT-C to the recipient myocardium was assessed by immunohistochemistry of EECT-C-transplanted hearts. Before implantation, EECT-C was transduced with adenovirus encoding GFP to distinguish between transplanted cells and recipient myocardium. Images reveal plentiful Cx43 (white arrows) at the boundary between the EECT-C and the epicardium (**Figure 6**). Taken together, the in vitro and in vivo functional and immunohistochemistry data support the notion that the functional A-V conduction by EECT-C is mediated by electrical coupling through Cx43 gap junctions. Nevertheless, we cannot conclusively rule out the possibility that the coupling is at least partly mechanical (24,25).

DISCUSSION

Current therapies for myocardial conduction blocks depend on electronic devices to deliver electrical pulses downstream of the region of the block (26). Although effective, it would be desirable to restore conduction or bypass areas of slow conduction by regenerating injured myocardium or by implanting an artificial conduction tract. As an alternative to devices and ablative therapies, we engineered de novo electrical conduction tracts capable of bridging myocardial regions of slow conduction or conduction block (**Central Illustration**).

The ability of isolated ventricular myocytes in culture to spontaneously organize into 3-dimensional structures has long been recognized (27). Moreover, a number of 3-dimensional tissue culture techniques were developed as biological systems for studying cell-cell interactions, electrical coupling, and extracellular matrix interactions (28-30). Various scaffold-based approaches using different polymers have been utilized. The ability of skeletal myoblast-based tissue constructs to restore AV conduction in the rat heart was first described by Choi et al. (31). Using a silicone cast, the investigators fabricated small tissue constructs made from a myoblast Matrigel-based solution that were subsequently transplanted into the rat heart (31,32). In addition, Kirkton and Bursac (33) engineered 3-dimensional cardiac tissue cords consisting of NRVMs and gene-modified HEK293 cells. Although the use of transformed HEK293 cells

FIGURE 5   Restoration of AV Block by In Vivo Implantation of EECT

(A) QRS interval duration and **(B)** PR interval duration in EECT-C10-implanted animals compared with control animals. **Bars** represent mean ± SEM; n = 3 animals per experimental group. *p < 0.05 by 2-sided Student *t* test. **(C)** Electrogram recordings of an EECT-C10-implanted heart both pre-infusion and post-methacholine infusion **(top panel),** and with atrial pacing during methacholine infusion, showing atrioventricular (AV) conduction **(bottom panel)**. **(D)** Recording during mechanical removal of EECT shows pacing deflection (P) followed by atrial depolarization (A) and no ventricular depolarization **(top panel)**. Recording during ventricular pacing (P) confirms ventricular depolarization (V), verifying viability of the ventricular myocardium **(bottom panel)**. ECG = electrocardiography; other abbreviation as in **Figures 2 and 4**.

diminished the immediate therapeutic potential of these constructs, gap junctional modification of the HEK293 cells changed the tissue construct's conduction properties in a predictable manner, providing an in vitro platform for studying cardiac conduction properties.

Our approach used a magnetic field to pattern an EECT composed of paramagnetic microspheres coated with cell-specific antibodies. As we showed with NRVMs and cardiac stromal cells, the flexibility

FIGURE 6   EECT-C Integration With the Recipient Myocardium
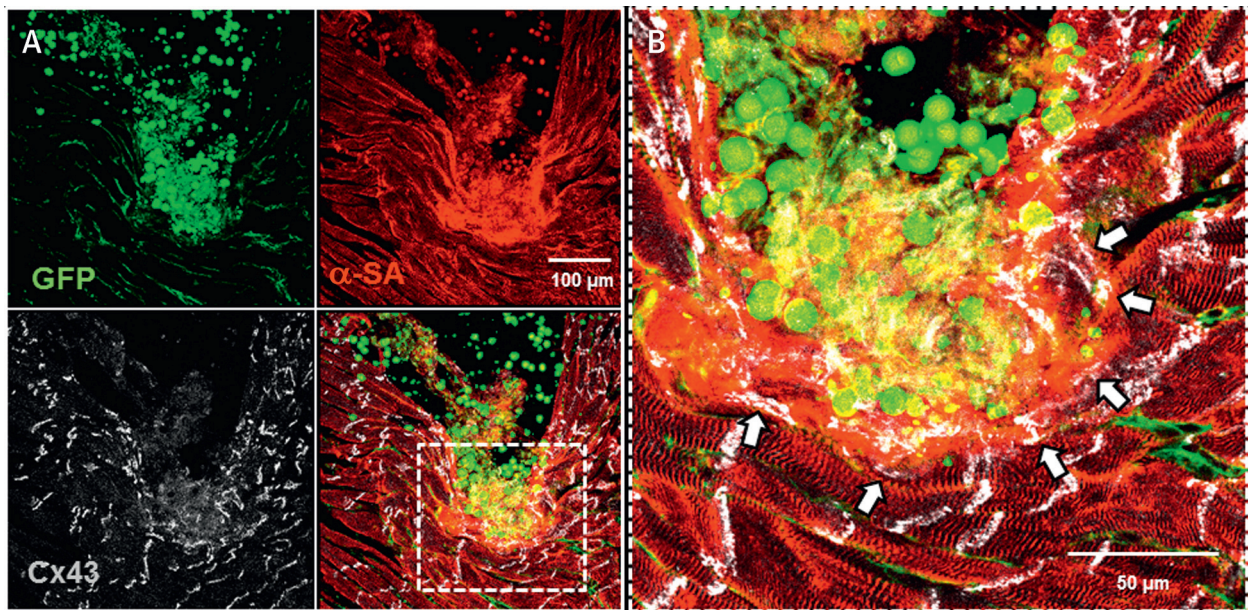
Immunohistochemistry of rat myocardium transplanted with EECT-C demonstrates connexin 43 (Cx43)-mediated gap junctions between the recipient myocardium and EECT-C. **(A) Green**: paramagnetic microspheres, manufactured to be green fluorescent, as well as NRVMs and CDCs transduced with an adenovirus-encoding green fluorescent protein (GFP) before implantation; **gray**: Cx43; **red**: α-sarcomeric actinin (SA). **Bottom right**: merged image of GFP, α-SA, and Cx43. **(B)** Enlargement, demonstrating the presence of Cx43 **(white arrows)** between EECT-C and the recipient myocardium. Abbreviations as in **Figures 1, 2, and 4**.

to conjugate microspheres with different antibodies provides a generalizable platform to engineer EECTs with specific electrophysiological and/or structural properties. Affinity binding between paramagnetic beads and ventricular myocytes was mediated by gamma-sarcoglycan, a surface antigen robustly expressed on cardiomyocytes, including those of human origin (34,35). Thus, although we did not test the theory here, we anticipate that EECTs constructed with human pluripotent stem cell-derived cardiomyocytes would exhibit similar functionality as those constructed with NRVMs. The addition of cardiac stromal cells increased the structural integrity of the EECTs and yielded more consistent conduction properties. Our data demonstrate the ability of the 3-dimensional tissue structure to restore cardiac electrical conduction in an in vitro model of conduction block and by implanting a pre-formed EECT-C, in vivo followed by in vivo and ex vivo electrophysiological recordings.

Downstream of the AV node, the cardiac conduction system is electrically insulated, preventing electrical propagation from dissipating laterally into the surrounding myocardium (36,37). Likewise, end-to-end electrical propagation along the run of the EECT without lateral flux would be desirable to maximize signal fidelity and help overcome impedance mismatch. Our data showed that the EECT constructs transplanted in vivo faithfully relayed atrial activation to the ventricle (**Figure 5**), indicating that lateral "signal loss" was insignificant. Only the terminal ends of the EECT were fibrin-glued to the myocardium; physical adhesions of the EECT elsewhere may eventually form. Complete electrical insulation of EECT may be challenging because acellular structures such as microtubules can mediate electrical coupling (38). Nonetheless, our approach to tissue patterning with paramagnetism and carefully chosen cell surface antigens is amenable to creating insulating layers (should such insulation be required) composed of poorly coupled cells, such as dermal fibroblasts (39) above and beneath the EECTs.

Other than the use of fibrin glue, no treatment was performed to attach the EECT onto the epicardial surface. Fibrin glue provides scaffolding for cardiac tissue engraftment (40), promotes angiogenesis (41), and mediates nerve regeneration by providing a

CENTRAL ILLUSTRATION Implantation of EECT Restores AV Conduction in Complete Heart Block
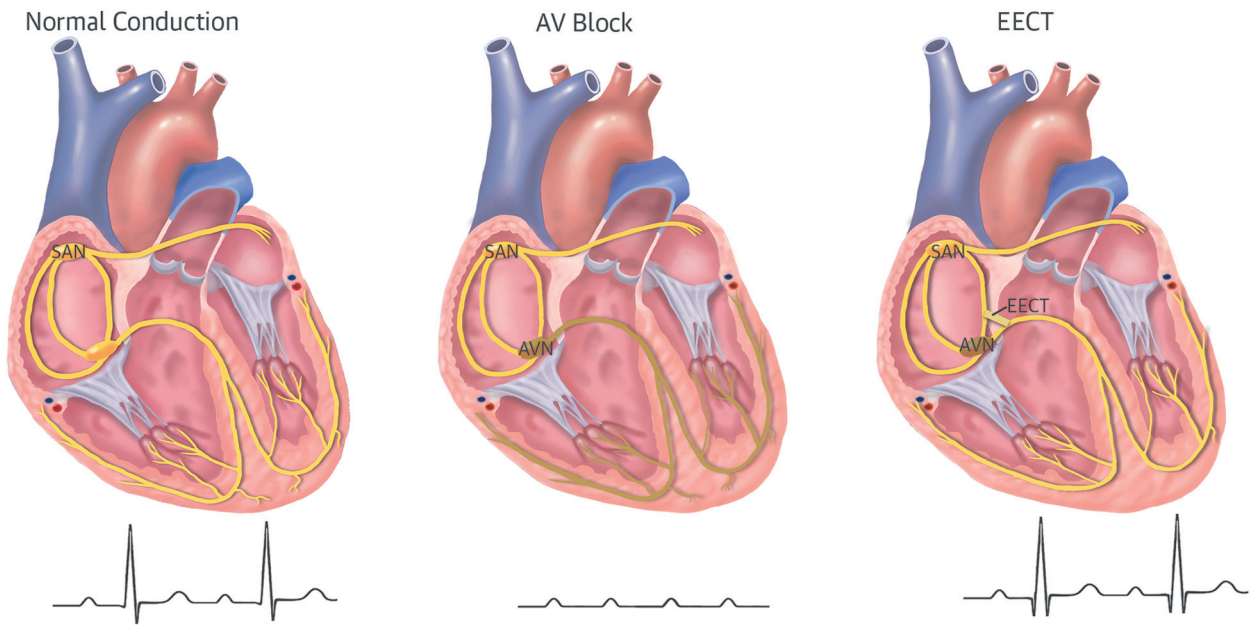
Cingolani, E. et al. J Am Coll Cardiol. 2014; 64(24):2575–85.

Normal conduction **(left panel)** initiated in the right atrium (P waves) travels across the atrioventricular (AV) node to the ventricles (QRS complexes). In AV block **(central panel)**, atrial conduction (P waves) cannot reach the ventricular myocardium (absence of QRS complexes). Implantation of EECT **(right panel)** restores AV conduction in complete heart block.

favorable matrix microenvironment (42). Because the EECT ends were affixed to the myocardium at the time of surgery, and Cxs turn over rapidly (1.5 to 5 h) (11,12), a 3-day window would be sufficient for establishing gap junctional and/or acellular electrical coupling (38) of the EECT termini to the myocardium. The presence of Cxs at the border between the EECT-C and the epicardium 3 days after EECT-C transplantation in vivo further supports electrical coupling of EECT-C to the host myocardium, although a role for mechanotransduction cannot be excluded (24,25).

Spontaneous contraction of the EECT (Online Video 1) arises from occasional self-excitability of some NRVMs, driving contraction of the entire construct, as we observed in the NRVM monolayers (17). The rate of these occasional contractions is much lower (~100 beats/min) than the sinus rate of the rat (~320 beats/min). Thus, sinus rhythm is expected to entrain spontaneous contraction of the EECT-C upon implantation in vivo. The EECT is optically thin, with no more than ~5 layers of cells in its short axis. Although we did not directly examine the long-term

viability of the EETCs, such thin structures are expected to remain viable via soluble gas exchange without dedicated vasculature. Multiple lines of evidence support this notion: 1) myoglobin-facilitated oxygen diffusion mechanisms are sufficient to oxygenate the rat myocardium when cellular oxygen falls low (43); and 2) diffusion coefficients of oxygen in muscle fibers (1.1×10^{-4} to 4×10^{-8} cm^2/s) (44,45) are sufficient to cover the cross-sectional dimensions of the EECT.

STUDY LIMITATIONS. As electrical conduction propagates along the EECT, it encounters a highly hyperpolarizing, electrical sink at the EECT–ventricular myocardium interface. This is akin to the source-sink mismatch in the sinoatrial node surrounded by the hyperpolarizing atrial myocardium. The sinoatrial node solves this problem by populating its pacemaker cells with Cx45-expressing fibroblasts, thereby raising the input resistance (46). Similarly, incorporating relatively uncoupled CDCs (10) into EECTs should increase the input resistance, protecting the electrical source carried along the EECT-C10 from dissipation at the ventricular myocardium. Further

in vivo studies are warranted to test this notion. The low number of animals for the in vivo proof of concept experiments is a limitation of the present study.

The epicardial positioning of EECTs in the present study was purposely extravascular. Nevertheless, the paramagnetic microspheres used in this study were 8 μm in diameter, which may cause issues if released into the circulation. Although unlikely, this complication can be avoided in future constructs, as the present approach is amenable to smaller or biodegradable spheres, both of which are available commercially.

CONCLUSIONS

This proof of concept study showed that EECTs can re-establish cardiac electrical conduction between isolated regions of 2-dimensional cardiac tissue, as well as in the whole heart. Delivery and transplantation techniques need to be refined before translating this approach to large animal models. This technology could also be exploited for alternatives to open chest implantation, such as in situ EECT formation using transcutaneous or transesophageal electromagnetic probes to conglomerate tagged cells. The present approach is highly generalizable, offering a novel platform to engineer biocompatible materials for relaying electrical signals. A similar approach could be used, in principle, to bridge interrupted neural circuits in stroke, nerve, or spinal cord injuries.

REPRINT REQUESTS AND CORRESPONDENCE: Dr. Eduardo Marbán, Cedars-Sinai Heart Institute, 8700 Beverly Boulevard, Davis 1090, Los Angeles, California 90048. E-mail: eduardo.marban@cshs.org OR Dr. Hee Cheol Cho, Departments of Biomedical Engineering and Pediatrics, Emory University, 1760 Haygood Drive, HSRB E-184, Atlanta, Georgia 30322. E-mail: heecheol.cho@emory.edu.

PERSPECTIVES

COMPETENCY IN MEDICAL KNOWLEDGE: Although electronic pacemakers are presently used to manage patients with symptomatic bradycardia, engineered electrical conduction tracts could potentially create a substrate for restoring atrioventricular synchrony in those with atrioventricular nodal block.

TRANSLATIONAL OUTLOOK: Refined, less invasive delivery methods are needed to enable transplantation of engineered electrical conduction tracts capable of bypassing areas of conduction block, thereby restoring conduction at various levels of the cardiac conduction system and reducing the need for artificial electronic pacemakers.

REFERENCES

1. Pistolese M, Richichi G, Catalano V, Massini R. Electrocardiographic aspects of intermittent atrioventricular block in the phase of sinus rhythm. Cardiol Prat 1969;20:125–37 [in Italian].

2. Solligard E, Juel IS, Bakkelund K, et al. Gut luminal microdialysis of glycerol as a marker of intestinal ischemic injury and recovery. Crit Care Med 2005;33:2278–85.

3. Josephson ME. Clinical Cardiac Electrophysiology: Techniques and Interpretations. Philadelphia, PA: Lippincott Williams & Wilkins, 2008.

4. Wilkoff BL, Cook JR, Epstein AE, et al., Dual Chamber and VVI Implantable Defibrillator Trial Investigators. Dual-chamber pacing or ventricular backup pacing in patients with an implantable defibrillator: the Dual Chamber and VVI Implantable Defibrillator (DAVID) Trial. JAMA 2002;288: 3115–23.

5. Sweeney MO, Hellkamp AS, Ellenbogen KA, et al., MOde Selection Trial Investigators. Adverse effect of ventricular pacing on heart failure and atrial fibrillation among patients with normal baseline QRS duration in a clinical trial of pacemaker therapy for sinus node dysfunction. Circulation 2003;107:2932–7.

6. Stevenson WG, Soejima K. Catheter ablation for ventricular tachycardia. Circulation 2007;115: 2750–60.

7. Sacher F, Tedrow UB, Field ME, et al. Ventricular tachycardia ablation: evolution of patients and procedures over 8 years. Circ Arrhythm Electrophysiol 2008;1:153–61.

8. Komatsu Y, Daly M, Sacher F, et al. Endocardial ablation to eliminate epicardial arrhythmia substrate in scar-related ventricular tachycardia. J Am Coll Cardiol 2014;63:1416–26.

9. Sekar RB, Kizana E, Cho HC, et al. IK1 heterogeneity affects genesis and stability of spiral waves in cardiac myocyte monolayers. Circ Res 2009;104:355–64.

10. Smith RR, Barile L, Cho HC, et al. Regenerative potential of cardiosphere-derived cells expanded from percutaneous endomyocardial biopsy specimens. Circulation 2007;115:896–908.

11. Fallon RF, Goodenough DA. Five-hour half-life of mouse liver gap-junction protein. J Cell Biol 1981;90:521–6.

12. Beardslee MA, Laing JG, Beyer EC, et al. Rapid turnover of connexin43 in the adult rat heart. Circ Res 1998;83:629–35.

13. Heydemann A, McNally EM. Consequences of disrupting the dystrophin-sarcoglycan complex in cardiac and skeletal myopathy. Trends Cardiovasc Med 2007;17:55–9.

14. Hack AA, Ly CT, Jiang F, et al. Gamma-sarcoglycan deficiency leads to muscle membrane defects and apoptosis independent of dystrophin. J Cell Biol 1998;142:1279–87.

15. McNally EM, Passos-Bueno MR, Bonnemann CG, et al. Mild and severe muscular dystrophy caused by a single gamma-sarcoglycan mutation. Am J Hum Genet 1996;59:1040–7.

16. Er F, Larbig R, Ludwig A, et al. Dominant-negative suppression of HCN channels markedly reduces the native pacemaker current I(f) and undermines spontaneous beating of neonatal cardiomyocytes. Circulation 2003;107:485–9.

17. Kapoor N, Liang W, Marban E, et al. Direct conversion of quiescent cardiomyocytes to pacemaker cells by expression of Tbx18. Nat Biotechnol 2013;31:54–62.

18. Smith RR, Barile L, Messina E, et al. Stem cells in the heart: what's the buzz all about? Part 2: arrhythmic risks and clinical studies. Heart Rhythm 2008;5:880–7.

19. Camelliti P, Green CR, Kohl P. Structural and functional coupling of cardiac myocytes and fibroblasts. Adv Cardiol 2006;42:132–49.

20. Nag AC. Study of non-muscle cells of the adult mammalian heart: a fine structural analysis and distribution. Cytobios 1980;28:41–61.

21. Zak R. Development and proliferative capacity of cardiac muscle cells. Circ Res 1974;35 Suppl II:17–26.

22. Wellens HJ. Should catheter ablation be performed in asymptomatic patients with Wolff-Parkinson-White syndrome? When to perform catheter ablation in asymptomatic patients with a Wolff-Parkinson-White electrocardiogram. Circulation 2005;112:2201–7, discussion 2216.

23. Tonkin AM, Wagner GS, Gallagher JJ, et al. Initial forces of ventricular depolarization in the Wolff-Parkinson-White syndrome. Analysis based upon localization of the accessory pathway by epicardial mapping. Circulation 1975;52:1030–6.

24. Starzl TE, Hermann G, Axtell HK, Marchioro TL, Waddell WR. Failure of sino-atrial nodal transplantation for the treatment of experimental complete heart block in dogs. J Thorac Cardiovasc Surg 1963;46:201–5.

25. Quinn TA, Kohl P. Mechano-sensitivity of cardiac pacemaker function: pathophysiological relevance, experimental implications, and conceptual integration with other mechanisms of rhythmicity. Prog Biophys Mol Biol 2012;110:257–68.

26. Epstein AE, DiMarco JP, Ellenbogen KA, et al., American College of Cardiology Foundation; American Heart Association Task Force on Practice Guidelines; Heart Rhythm Society. 2012 ACCF/AHA/HRS focused update incorporated into the ACCF/AHA/HRS 2008 guidelines for device-based therapy of cardiac rhythm abnormalities: a report of the American College of Cardiology Foundation/American Heart Association Task Force on Practice Guidelines and the Heart Rhythm Society. J Am Coll Cardiol 2013;61:e6–75.

27. Halbert SP, Bruderer R, Lin TM. In vitro organization of dissociated rat cardiac cells into beating three-dimensional structures. J Exp Med 1971;133:677–95.

28. Desroches BR, Zhang P, Choi BR, et al. Functional scaffold-free 3-D cardiac microtissues: a novel model for the investigation of heart cells. Am J Physiol Heart Circ Physiol 2012;302:H2031–42.

29. Radisic M, Park H, Gerecht S, et al. Biomimetic approach to cardiac tissue engineering. Philos Trans R Soc Londo B Biol Sci 2007;362:1357–68.

30. Liau B, Zhang D, Bursac N. Functional cardiac tissue engineering. Regen Med 2012;7:187–206.

31. Choi YH, Stamm C, Hammer PE, et al. Cardiac conduction through engineered tissue. Am J Pathol 2006;169:72–85.

32. Sill B, Alpatov IV, Pacak CA, Cowan DB. Implantation of engineered tissue in the rat heart. J Vis Exp 2009 Jun 24:1139–40.

33. Kirkton RD, Bursac N. Engineering biosynthetic excitable tissues from unexcitable cells for electrophysiological and cell therapy studies. Nat Commun 2011;2:300.

34. Hack AA, Groh ME, McNally EM. Sarcoglycans in muscular dystrophy. Microsc Res Tech 2000;48:167–80.

35. Wheeler MT, Allikian MJ, Heydemann A, et al. Smooth muscle cell-extrinsic vascular spasm arises from cardiomyocyte degeneration in sarcoglycan-deficient cardiomyopathy. J Clin Invest 2004;113:668–75.

36. Atkinson A, Inada S, Li J, et al. Anatomical and molecular mapping of the left and right ventricular His-Purkinje conduction networks. J Mol Cell Cardiol 2011;51:689–701.

37. Wessels A, Markman MW, Vermeulen JL, et al. The development of the atrioventricular junction in the human heart. Circ Res 1996;78:110–7.

38. Kohl P, Gourdie RG. Fibroblast-myocyte electrotonic coupling: does it occur in native cardiac tissue? J Mol Cell Cardiol 2014;70:37–46.

39. Kizana E, Ginn SL, Allen DG, et al. Fibroblasts can be genetically modified to produce excitable cells capable of electrical coupling. Circulation 2005;111:394–8.

40. Christman KL, Fok HH, Sievers RE, et al. Fibrin glue alone and skeletal myoblasts in a fibrin scaffold preserve cardiac function after myocardial infarction. Tissue Eng 2004;10:403–9.

41. Bach TL, Barsigian C, Chalupowicz DG, et al. VE-cadherin mediates endothelial cell capillary tube formation in fibrin and collagen gels. Exp Cell Res 1998;238:324–34.

42. Choi BH, Han SG, Kim SH, et al. Autologous fibrin glue in peripheral nerve regeneration in vivo. Microsurgery 2005;25:495–9.

43. Lin PC, Kreutzer U, Jue T. Myoglobin translational diffusion in rat myocardium and its implication on intracellular oxygen transport. J Physiol 2007;578:595–603.

44. Krogh A. The rate of diffusion of gases through animal tissues, with some remarks on the coefficient of invasion. J Physiol 1919;52:391–408.

45. MacDougall JD, McCabe M. Diffusion coefficient of oxygen through tissues. Nature 1967;215:1173–4.

46. Camelliti P, Green CR, LeGrice I, et al. Fibroblast network in rabbit sinoatrial node: structural and functional identification of homogeneous and heterogeneous cell coupling. Circ Res 2004;94:828–35.

KEY WORDS arrhythmias, cardiac tissue engineering, gap junctions, heart conduction system

---

APPENDIX For a supplemental figure as well as a supplemental video and its legend, please see the online version of this article.